

MEASURING THE EFFECT OF TENSION ON LIPID  
MEMBRANE VISCOSITY

by

MATTHEW REYER

A THESIS

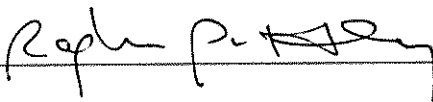
Presented to the Department of Physics  
and the Robert D. Clark Honors College  
in partial fulfillment of the requirements for the degree of  
Bachelor of Science

June 2015

## **An Abstract of the Thesis of**

Matt Reyer for the degree of Bachelor of Science  
in the Department of Physics to be taken June 2015

**Title:** Measuring the Effect of Tension on Lipid Membrane Viscosity

Approved:   
Dr. Raghuveer Parthasarathy

The fluidity of the lipid membrane is essential for many biological functions, such as cellular cargo trafficking and cell signaling. The timescale of this fluidity is dictated by the two-dimensional (2D) viscosity of the membrane. Membrane viscosity is poorly measured, and the effect of certain parameters on 2D membrane viscosity has not been tested, and is therefore unknown. The purpose of this research is to explore the effect of one of those parameters: tension. Examples of cellular membranes under tension include the membranes of cells involved in cell crawling or the membranes of cells involved in the Notch signaling pathway.

In order to study the effect of tension on lipid membranes, I examined cell-free, model lipid membranes. I built and used a micropipette aspiration system and observed diffusion in phase-separated Giant Unilamellar Vesicles (GUVs). Micropipette aspiration is a technique in which lipid vesicles are partially suctioned into pipettes of a few microns in diameter, stretching the membrane and inducing tension.

The results of the experiment indicate that membrane viscosity decreases with increased tension. This provides the first measurement of tension-mediated viscosity changes, which opens the door to many future experiments.

## **Acknowledgements**

I would like to thank Professor Raghu Parthasarathy for welcoming me into his lab and for being my scientific mentor for the past two years. I have no doubt that I would not be where I am today, and that my future would be on much shakier grounds, if not for his guidance.

I would also like to thank Tristan Hormel for introducing me to the world of lipid membrane biophysics, for his programming expertise, and for being a generally enjoyable person to work next to. Thanks Tristan, our conversations were generally enjoyable.

I would also like to thank my parents, Mark and Barb, for putting up with me and for their exemplary upholding of the typical parenting duties.

And finally, I would like to thank Mr. Matt Price of Lakeridge High School. If Mr. Price ever reads this, I would like him to know it was he who inspired me to pursue physics.

## Table of Contents

Chapter 1: Introduction	1
1.1 Lipid Bilayers	1
1.2 Two-Dimensional Viscosity	2
1.3 A Brief Note on the Two-Dimensionality of Lipid Membranes	5
1.4 Lipid Membranes under Tension	6
1.5 Tension Hypothesis	7
Chapter 2: Experimental Methods	9
2.1 Giant Unilamellar Vesicles	9
2.1.1 Phase Separation	10
2.2 Micropipette Aspiration	13
2.3 Experimental Set-Up	15
2.3.1 Adjustable Water Reservoir	15
2.3.2 Two-Way Valve with Reservoir	18
2.3.3 Micromanipulator	19
2.3.4 Making Pipettes	19
2.3.5 Filling and Coating Pipettes	20
2.4 Microrheology and Image-Based Tracking	23
Chapter 3: Results and Discussion	26
3.1 Verification of Experimental Approach	26
3.2 Average Domain Radius and Diffusion Coefficient versus Tension	26
3.3 Viscosity versus Membrane Tension	28
3.4 Conclusions and Implications	29
Appendix A: Making Giant Unilamellar Vesicles	31

## **List of Figures**

Figure 1: Lipid Bilayer Illustration by Raghuv eer Parthasarathy	1
Figure 2: Two Examples of Two-Dimensional Fluids	5
Figure 3: Two Phase-Separated GUVs	11
Figure 4: Schematic of Aspirated Phase-Separated, Giant Unilamellar Vesicle	14
Figure 5: Adjustable Water Reservoir	16
Figure 6: GUVs on a Glass Slide with Micropipette in Place	17
Figure 7: Water Reservoir in Equilibrium Pressure Position	17
Figure 8: Hydrostatic Pressure Calculation	18
Figure 9: Vacuum Filling System for Micropipettes	22
Figure 10: Three-Well Chamber for Filling Pipettes	22

# Chapter 1: Introduction

## 1.1 Lipid Bilayers

The cell membranes of most living organisms are made of lipid bilayers. A lipid bilayer, as the name suggests, consists of two sheets of lipids. Lipids are naturally-occurring molecules which include fats, sterols, phospholipids, etc. All lipids in lipid bilayers have a hydrophilic head group and a hydrophobic tail group, meaning that the heads of the lipids are attracted to water, and the tails of the lipids are repelled by water. Therefore, when placed in water, lipids naturally line up in two layers, with heads facing out and tails facing each other (see Figure 1).

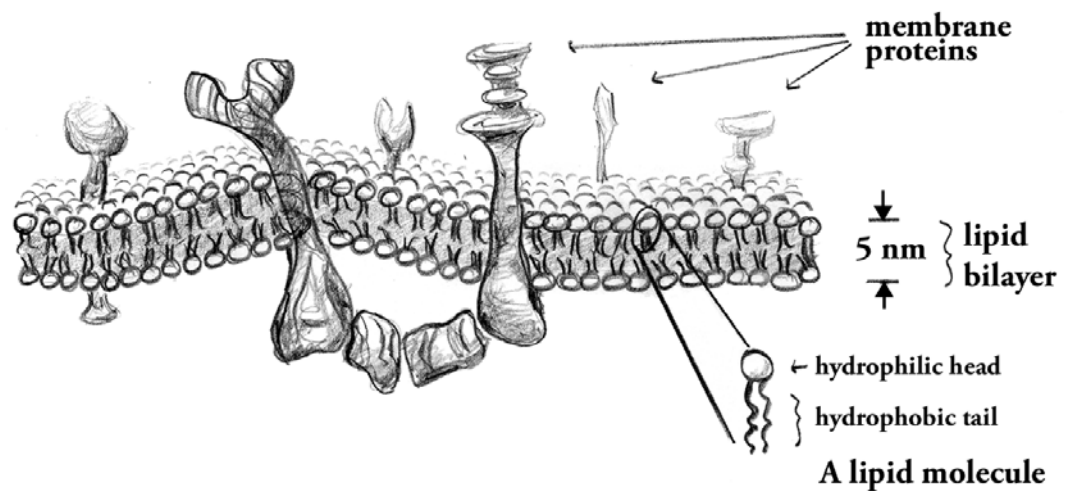


Figure 1: Lipid Bilayer Illustration by Raghuvveer Parthasarathy

Lipids, which consist of hydrophilic heads and hydrophobic tails, naturally form bilayers when placed in water. Lipid bilayers form the cell membranes of most living organisms.

In addition to lipids, cell membranes also include embedded membrane proteins.

Together, lipids and membrane proteins each form about half of the cell membrane.

Lipid bilayers typically contain several types of lipids, each with its own physical property [1]. Lipid bilayers have both passive and active roles in cell function. Because of the hydrophobic nature of their tails, lipid layers are impermeable to water-soluble molecules such as ions, proteins, and sugars, making the lipid bilayer the ideal membrane barrier for the cell and its organelles [2]. More actively, lipid bilayers are involved in cell signaling, cell division, and cellular cargo transport [1,3,4].

All these active processes of the lipid membrane involve the motion of lipids and proteins, and the bending of the membrane, implying that the lipid membrane is not a solid or rigid structure, but rather a fluid. Indeed, it was the fluid mosaic model of Singer and Nicolson which first described biological membranes as two-dimensional (2D) fluids in which lipids and proteins can diffuse [5]. It is this fluidity which allows for these active processes of the lipid bilayer, and therefore it is patently important for cell function and biology in general. Therefore, it is of great interest and import to characterize the physical parameters of this 2D fluid. The parameter of particular interest in this paper is the 2D viscosity of the lipid membrane, as it is the 2D viscosity which controls how fast lipid motion occurs, and consequently, the 2D viscosity sets the timescale for many important cell functions.

## **1.2 Two-Dimensional Viscosity**

Viscosity is a measure of a fluid's resistance to flow or deform. The higher the viscosity of a fluid, the more force it takes for things to move in it. Water has a lower viscosity than, for example, honey or molasses. In the context of lipid membranes, the higher the viscosity, the slower lipids move around. Our ability to accurately model many cellular processes depends on our ability to measure the 2D viscosity of the lipid

membrane, for it is the 2D viscosity which sets the timescale for those functions which depend on lipid and protein motion.

Unfortunately 2D viscosity is difficult to measure and remains poorly quantified, especially compared to the typical three-dimensional (3D) viscosity, which is commonly and easily measured. Whereas tools exist to directly measure the 3D viscosity of liquids, 2D viscosity must be calculated indirectly by first measuring the diffusion along the membrane. Diffusion is the random motion of molecules, driven by ambient thermal energy. This motion is characterized by “random walks.” While each “step” of a diffusing particle is random, by observing many diffusing particles over time, statistics can be used to quantify the diffusive motion.

Diffusion of lipids can be observed experimentally, and mathematical models exist which derive 2D viscosity from the numbers associated with that diffusion. The first relevant equations are the Einstein relations, which describe the relation between the diffusion coefficients of lipids and their corresponding drag coefficients. The Einstein relations are:

$$(1) \mathbf{D}_R = \mathbf{k}_B \mathbf{T} \mathbf{b}_R$$

$$(2) \mathbf{D}_T = \mathbf{k}_B \mathbf{T} \mathbf{b}_T$$

where  $\mathbf{D}_R$  and  $\mathbf{D}_T$  refer to the rotational and translational diffusion coefficients, respectively. For lipids, rotational diffusion refers to the motion around its head-to-tail axis, and translational diffusion refers to its motion along the plane of the membrane.  $\mathbf{T}$  is the temperature of the fluid,  $\mathbf{k}_B$  is Boltzmann’s Constant, and  $\mathbf{b}_R$  and  $\mathbf{b}_T$  refer to the rotational and translational drag coefficients, respectively. The diffusion coefficients can be determined experimentally. Boltzmann’s constant and temperature are both

known, and the drag coefficients are derived from the other variables. With the drag coefficients, we can solve for 2D viscosity by using one of two models: the Saffman-Delbrück model, or the Hughes, Pailthorpe, White (HPW) model [6,7]. The Saffman-Delbrück model is as follows:

$$(3) \mathbf{b}_T = \frac{(4\pi\eta_m)}{\ln(2\epsilon^{-1}) - \gamma}$$

$$(4) \mathbf{b}_R = 4\pi\eta_m \mathbf{a}^2$$

where  $\mathbf{a}$  is the membrane inclusion radius, i.e. the radius of the moving patch of lipids or proteins,  $\gamma$  is Euler's constant,  $\epsilon$  is a ratio relating the viscosity of the membrane, the viscosity of the fluid surrounding it (bulk viscosity), and  $\mathbf{a}$ , and finally,  $\eta_m$  is the viscosity of the membrane, the value we are trying to determine. The Saffman-Delbrück model applies for systems with small  $\epsilon$ , i.e. high membrane viscosities. The HPW model extends the Saffman-Delbrück model to diffusing objects of any inclusion radius. The equations however, are much more complicated than the Saffman-Delbrück equations, and can only be solved numerically.

The Saffman-Delbrück equations provide the framework by which we can get from observed diffusion to 2D estimates. Mathematically, the process is straightforward. Experimentally, the process becomes more complicated. Furthermore, it is unknown how certain parameters affect the 2D viscosity of lipid membranes. One of these untested parameters, the one which this paper will focus on, is tension. There are real-life scenarios in which lipid membranes are subjected to heightened tension, and the goal of this project is to see if tension has any effect on membrane viscosity and, therefore, the motion of membrane molecules.

### 1.3 A Brief Note on the Two-Dimensionality of Lipid Membranes

Much emphasis has been placed on the lipid membrane being a two-dimensional fluid. How accurate is this? Most fluids we encounter in everyday life are three-dimensional; it is, in fact, odd to imagine a 2D fluid.

While it is true that there exist a non-zero number of atoms between the two layers of lipid heads in a bilayer, in all, the bilayer is no more than five nanometers in thickness (see Figure 1). Additionally, there is no space between the tails of the two lipid layers, not even for water, due to the hydrophobic nature of the tails. The lipid bilayer is as two-dimensional as possible in biology. Another example of a 2D fluid is a soap film which, unlike a lipid bilayer, actually has space for water in between its two layers of molecules (see Figure 2).

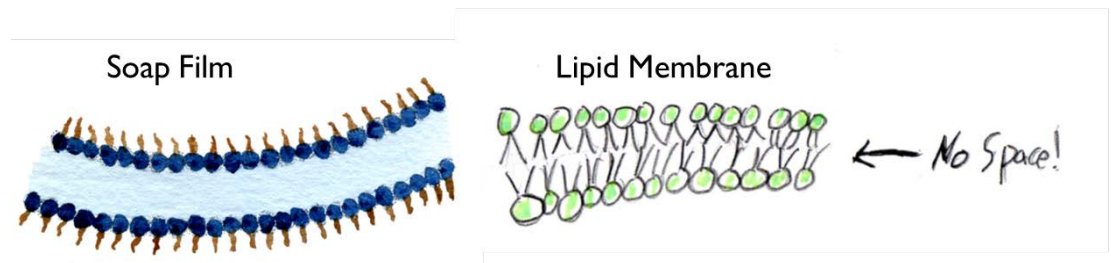


Figure 2: Two Examples of Two-Dimensional Fluids

Unlike a soap film, there is no space between the two layers of molecules in a lipid bilayer. The lipid bilayer is as two-dimensional as it gets in biology.

Furthermore, and perhaps most importantly, the lipid motion we are concerned about occurs *in the plane* of the lipid layer. Diffusion of particles *across* the membrane is not relevant to this experiment. A single monolayer of lipids is on the scale of 1-2 nanometers in thickness, and it behaves fundamentally differently than a three-dimensional fluid.

#### **1.4 Lipid Membranes under Tension**

As mentioned earlier, there are real-life scenarios in which lipid membranes might be subjected to tension. For example, it is believed that cell crawling, which occurs during wound healing and cancer metastasis, is controlled by membrane tension. During cell crawling, a cell attaches to a surface, detaches and projects an extension of its membrane, called a lamellipodium, and then reattaches at a point further along the surface. It has been shown that the rate at which the lamellipodium extends and consequently the rate at which cells crawl is controlled by membrane tension [8,9]. Additionally, the tension and tension distribution is believed to be fundamentally different between stationary cells and moving cells [10]. Cells can crawl without any external force driving the motion. In order to do this, they can actually alter their tension in order to stretch.

Cells are able to create polarized distributions of signaling molecules along their membranes, and this polarized distribution is necessary for biological processes such as cell division, neurite formation, and cell motility. It was once believed that the polarized distribution of signaling molecules, rather than a uniform distribution, was controlled by diffusible molecules in the protruding edge of the cell membrane. Recently, though, the Weiner Lab at University of California, San Francisco found that membrane tension doubled in the protruding edge of the cell membrane, and that reducing membrane tension led to a uniform distribution of signaling molecules. This suggested that it was in fact tension, not diffusible molecules, which was responsible for cell polarity, and therefore is an important factor in these cellular processes [11].

Membrane tension can also serve as a means by which cells and bacteria detect forces being applied to them. Mechanosensors are molecules which respond to changes in mechanical force. Bacteria contain two families of mechanosensitive channels, one of which, MscL, is highly conserved. The MscL channel activates when it senses a change in force. There are many avenues, though, through which a force can be changed. It is now known that the MscL channel detects force changes by sensing the tension in the membrane. It is also possible that tension is also the stimulus behind eukaryotic Mechanosensors [12].

Many of these processes (cell crawling, signaling, etc.) are known to also be influenced by membrane viscosity. Therefore, it seems that membrane tension and viscosity are simultaneously significant factors in many processes. It would therefore be interesting to know the influence the two variables have on each other, if any. This question, whether or not tension affects membrane viscosity, is the focus of this paper.

### **1.5 Tension Hypothesis**

My hypothesis is that high tension will lead to lower membrane viscosity. Increasing tension should stretch out the lipid membrane, leading to more space between the lipids, which will allow for the lipids to move more easily. If the lipids move more quickly, then the diffusion coefficients referred to in equations (1) and (2) will be higher, which would produce lower viscosity values.

In order to test this hypothesis, I use a technique called micropipette aspiration on lipid vesicles. Lipid vesicles are model systems. Cell membranes are complex, but lipid vesicles are made of a controlled lipid composition and are similar in size to cells. Micropipette aspiration is a technique in which lipid vesicles are suctioned partially into

small, glass pipettes ( $\sim 1-5 \mu\text{m}$  in radius). This suction stretches out the membrane of the vesicle, creating tension. I built the micropipette aspiration device used in my experiments, and developed many of the experimental techniques. The device and techniques will continue to be used in future experiments involving tension on vesicles.

## Chapter 2: Experimental Methods

### 2.1 Giant Unilamellar Vesicles

The vesicles I use in this experiment are called phase-separated Giant Unilamellar Vesicles (GUVs). In biology, the term vesicle refers to a lipid bilayer which has been rolled up into a sphere. It is essentially a hollow, spherical shell made of a lipid bilayer. The vesicles I use for micropipette experiments are artificial, but there are natural lipid vesicles with real biological functions. GUVs serve as an idealized, cell model. The advantages of using artificial vesicles are that we can control their size and composition, and can create numerous (roughly) similar vesicles at the same time.

Unilamellar means that there is a single wall of lipid bilayer in this vesicle. Other model systems might be multilamellar, which means there are many lipid bilayers stacked on top of each other. On average, GUVs are around 20-50 microns ( $\mu\text{m}$ ) in size.

On the inside and outside of the lipid bilayers is a fluid meant to represent the intra- and extracellular fluid a real cell would typically be surrounded by. In this case, the fluid is a 0.1 Molar sucrose solution. GUVs are compositionally and structurally similar to a cell membrane without all the subcellular components. Therefore, tension experiments on GUVs are a simple analogue for tension experiments on real cells.

GUVs are formed by electroformation. First, a mixed-lipid composition is deposited onto heated Indium Tin Oxide (ITO) coated glass slides. The lipids are then dehydrated in a vacuum chamber for thirty minutes. After the vacuum chamber, the glass slides are stuck together with lipid sides facing each other and a small piece of Teflon placed in between to create a capacitor, which is then attached to a function

generator. The function generator outputs a sinusoidal alternating current for around three hours [13, 14].

The lipid compositions I use to form the GUVs consist of 1,2-dipalmitoyl-sn-glycero-3-phosphocholine (DPPC), 1,2-dioleoyl-sn-glycero-3-phosphocholine (DOPC), and cholesterol. DPPC, DOPC, and cholesterol are all lipids. The ratios of DPPC, DOPC, and cholesterol in the lipid compositions vary, with the concentration of each individual lipid typically in the range of 20 to 40% of the total lipid mixture. In addition to those three lipids, we also include a biotinylated lipid, which allows the membrane to bond to a tracer particle if need be, and a fluorescent lipid probe (Texas Red DHPE), which is what allows us to see the actual GUVs under a microscope. Both the biotinylated lipid and the Texas Red DHPE typically make up about one percent of the composition.

Though I have used many different compositions for vesicles in the past, with both DOPC-dominant and DPPC-dominant compositions, I used a 2:1 DPPC:DOPC, 40 percent cholesterol, composition for the entirety of my micropipette experiments. I used only one composition because although the viscosity values would certainly change for different compositions, the overall relationship between membrane tension and viscosity should not depend on the composition.

### *2.1.1 Phase Separation*

In order to extract viscosity numbers we first need to observe diffusion to obtain values for diffusion coefficients. Observing GUVs alone does not allow us to quantify viscosity, because we are looking for motion on the membrane of the vesicle, and the heads of lipids all look the same. It is impossible to track the motion of a lipid if it is

identical to its background. In order to solve this problem, I exploit the phenomenon of phase-separation.

“Phase” refers to the phases of matter, such as the familiar gas, liquid, and solid. The important phases in mixed-lipid membranes are the liquid-ordered and liquid-disordered phases. At room temperature, DOPC exists in the liquid-disordered phase, and DPPC exists in the liquid-ordered phase. In the presence of cholesterol, the two different phases separate, and the lesser-concentrated lipids self-assemble into circular, liquid domains [14, 15, 16]. The Texas Red fluorescent dye included in the GUV composition binds differently to the two different phases, resulting in differently-colored lipid domains. For the 2:1 DPPC:DOPC GUVs I use in these experiments, the final result is a dark colored vesicle with bright, circular domains (see Figure 3, below).

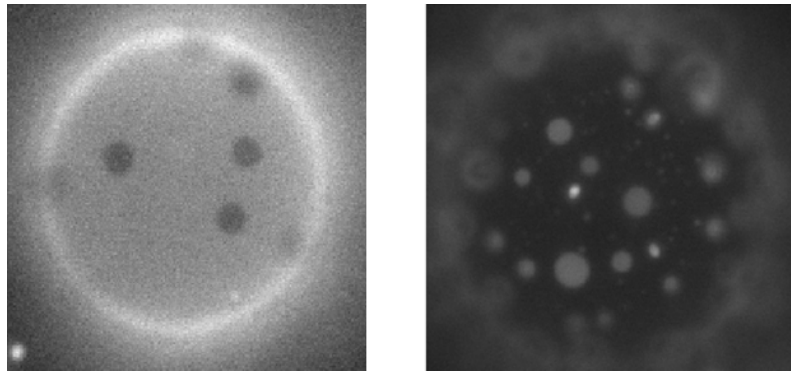


Figure 3: Two Phase-Separated GUVs

Left: 2:1 DOPC:DPPC, 20% Cholesterol GUV exhibiting phase-separation. The dark domains are DPPC, in the liquid-ordered phase

Right: 2:1 DPPC:DOPC, 40% Cholesterol GUV exhibiting phase-separation. The light domains are DOPC, in the liquid-disordered phase. This is the composition I use in my experiments.

Using a fluorescent microscope, we can see these GUVs and the individual lipid domains. The lipid domains exhibit diffusive motion, so they are the objects that allow us to observe diffusion in the bilayer. Using the diffusion numbers of those lipid domains, which are derived experimentally, we can glean information on the viscosity of the membrane using equations (3) and (4).

One convenient feature of phase-separated GUVs is that they provide all the information needed to solve equations (3) and (4) for viscosity. Generally, there are two scenarios. In order to solve the two equations, (3) and (4), for membrane viscosity, there can be at most two unknowns including the viscosity. In one scenario, we can calculate both the rotational and translational diffusion coefficients, in which case the two unknowns are the viscosity,  $\eta_m$ , and the inclusion radius,  $a$ . The Parthasarathy lab has done experiments in the past using paired fluorescent beads, anchored to lipid membranes, as tracer particles in order to extract both the rotational and translational diffusion coefficients. The reason the inclusion radius is considered an unknown is that we cannot simply assume that the radius of the diffusing patch of lipids is the same as the radius of the tracer particles, due to interactions between the particle and the membrane which cannot be accurately quantified [17].

Fortunately, the inclusion radius in the case of phase-separated GUVs is just the radius of the lipid domain, which can be observed experimentally. With the inclusion radius known, we can skip the rotational equation (4) entirely, and solve for the membrane viscosity using only equation (3). So, using phase-separated GUVs and fluorescent microscopy, we can experimentally derive all the variables necessary to get from diffusion numbers to viscosity.

## **2.2 Micropipette Aspiration**

The question this thesis attempts to answer is whether or not tension has any effect on membrane viscosity. Micropipette aspiration is the process by which I apply tension to lipid vesicles. The mechanics of micropipette aspiration are conceptually simple, though challenging to implement. A small, glass pipette (~1-5 microns in radius) is attached by airtight tubing to a water reservoir. Adjusting the height of that water reservoir leads to a pressure difference at the tip of the pipette. That pressure difference can cause a flow into or out of the pipette and is the mechanism by which GUVs are drawn to the tip of the pipette. The GUV is then partially suctioned into the pipette, which stretches out the membrane of the vesicle, creating tension.

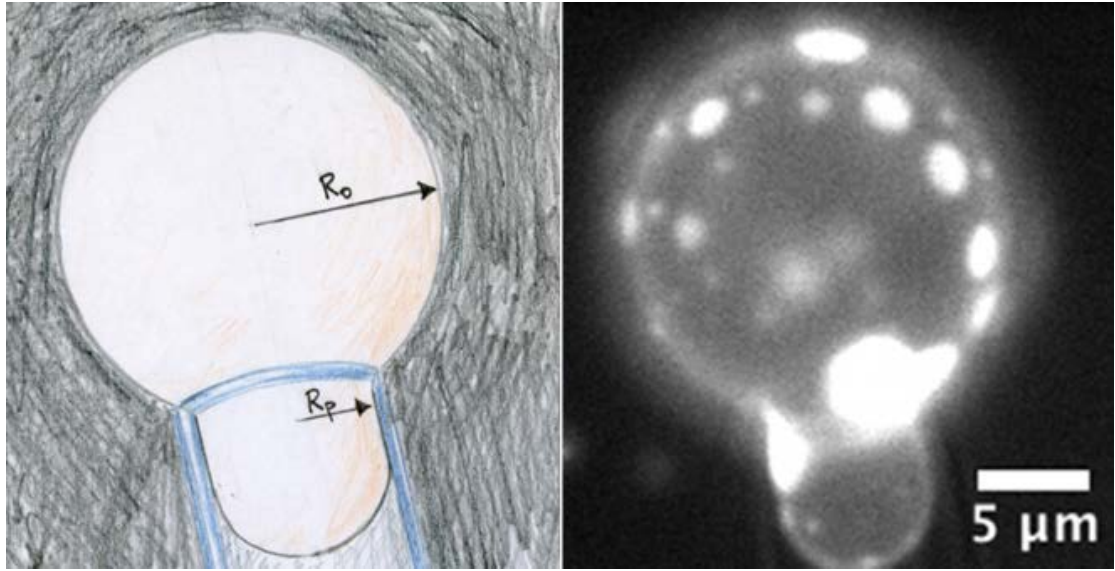


Figure 4: Schematic of Aspirated Phase-Separated, Giant Unilamellar Vesicle

A schematic of an aspirated GUV. To the left is a drawing by Raghu Parthasarathy representing the aspirated vesicle and the relevant parameters.  $R_p$  is the radius of the pipette.  $R_o$  is the radius of the vesicle outside the pipette (also called  $R_C$ ). To the right is an actual, experimental image of an aspirated GUV exhibiting phase separation.

From a still image of an aspirated vesicle (such as Figure 4, above), the membrane tension can be calculated. Derived from the Laplace Pressure, the equation which gets us from pressure and the geometry of the pipette and vesicle to a value for tension is:

$$(5) \Delta P = 2T_C \left( \frac{1}{R_P} - \frac{1}{R_C} \right)$$

Where  $\Delta P$  is the pressure difference accounted for by the change in height of the water reservoir (original pressure,  $P_0$ , is set at equilibrium),  $R_P$  is the radius of the pipette (and also the radius of the inner projection of the vesicle),  $R_C$  (also called  $R_O$  in Figure 4) is the radius of the vesicle outside the pipette, and  $T_C$  is the tension across the membrane of the vesicle [18, 19, 20].

## 2.3 Experimental Set-Up

In order to implement the procedure described above, I built a micropipette aspiration system. The components of that system are described in the following sections.

### 2.3.1 Adjustable Water Reservoir

The pressure control comes from an adjustable water reservoir. There are two levels of height control: a large, coarse control, and a small, fine control. The large, coarse control comes in the form of a meter-high metal slide, upon which the entire stage holding the water reservoir can be moved. The height on the large control can be measured to millimeter certainty.

The small, fine control is used when the stage holding the water reservoir is locked into place relative to the metal slide. Its height can be adjusted fractions of a millimeter at a time, and the exact height can be measured with tenth of a millimeter certainty. Pictures and schematics of the adjustable water reservoir can be seen below.

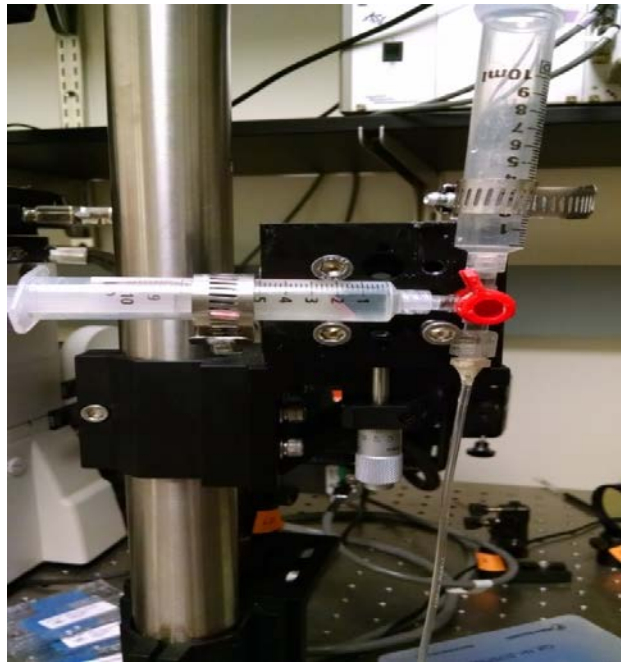


Figure 5: Adjustable Water Reservoir

The height of the water reservoir can be adjusted by either sliding the stage to which it is attached along the metal slide, or by turning the metal knob on the stage. Adjusting the metal slide creates large, but less precise, adjustments. Adjusting the stage itself using the metal knob allows small, precise adjustments.

GUV experiments are performed on a glass slide using a 60x magnification, contact objective on a fluorescent microscope (see Figure 6 below). Due to the short working distance of the contact objective, the tip of the micropipette must penetrate through the droplet of GUVs and come very close to the surface of the slide, within roughly one millimeter. Therefore, equilibrium pressure is considered to be when the surface of the water reservoir is even with the tip of the pipette (see Figure 7).



Figure 6: GUVs on a Glass Slide with Micropipette in Place

GUV experiments are performed using a glass slide and a 60x magnification, contact objective under a fluorescent microscope. The micropipette tip must penetrate the surface of the GUV solution, and come within a millimeter of the glass slide.

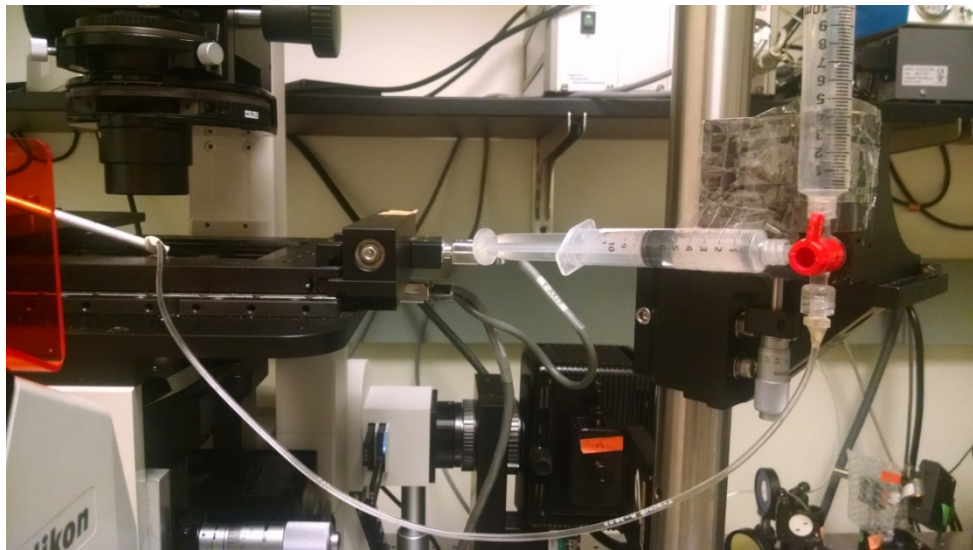


Figure 7: Water Reservoir in Equilibrium Pressure Position

At equilibrium, the surface of the water reservoir (in the vertical cylinder on the right) is even with the tip of the micropipette (on the left). The picture above actually shows the system slightly out of equilibrium, as the water reservoir is higher than the tip of the pipette.

The pressure applied to the vesicle comes from the hydrostatic pressure due to the vertical drop of the water reservoir, and is simply:

$$(6) \Delta P = \rho g \Delta h$$

Where  $\rho$  is the density of the fluid in the water reservoir (which is typically water, and therefore  $\rho = 1 \text{ g/mL}$ ),  $g$  is the gravitational acceleration,  $9.8 \text{ m/s/s}$ , and  $\Delta h$  is the height change of the water reservoir (see Figure 8, below).

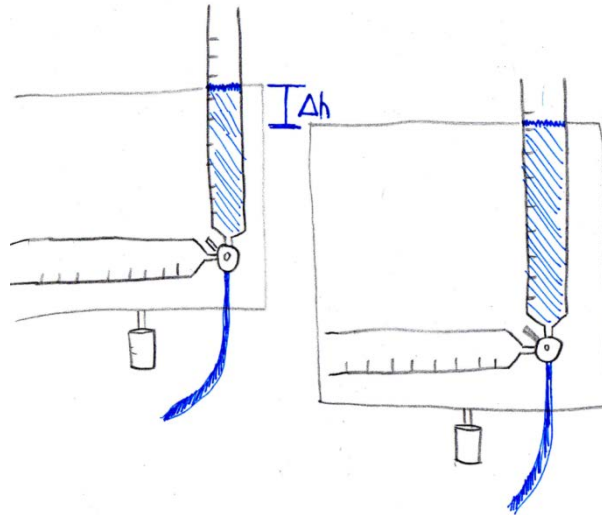


Figure 8: Hydrostatic Pressure Calculation

The hydrostatic pressure applied to the vesicle can be calculated simply using the height change of the water reservoir,  $\Delta h$ .

The hydrostatic pressure from the height change of the water reservoir is the same pressure we plug into equation (5), where we solve for membrane tension.

### 2.3.2 Two-Way Valve with Reservoir

In Figure 5, the two-way valve attached to the water reservoir is on display. The red knob can be turned to either create a path from the open-air, water reservoir to the pipette, or from a closed syringe to the pipette. The open-air, water reservoir provides

the hydrostatic pressure used in the experiment. The closed syringe can apply much larger forces, and can be used for a variety of reasons, such as clearing the pipette of any lipid residue which may have accumulated, or for drawing far away vesicles closer to the tip of the pipette.

### *2.3.3 Micromanipulator*

The micropipettes are held in place by a metal rod attached to a micromanipulator. The micromanipulator can move the pipette a few microns at a time on three axes. It is attached to the stage which holds the glass slide with the GUVs. It also holds pipettes in the vacuum device used for filling them (section 2.3.5)

### *2.3.4 Making Pipettes*

Micropipettes start as glass capillaries. The glass capillaries are made of borosilicate and have a 1.2 millimeter outer diameter, and a 1.0 millimeter inner diameter. Using a Sutter horizontal pipette puller, which applies heat and pulls the softened glass, the glass capillaries are made into closed pipettes, meaning that they have taken on a pipette shape, but the tip of the pipettes are closed. These are not useful in this experiment, as water needs to flow through the pipettes. The closed pipettes are turned into open pipettes using a microforge from World Precision Instruments. The microforge has a filament which can be heated up enough to melt the glass at the tip of the pipette. Using this function, the tip of the pipette is melted slightly and attached to the filament, which then retracts and breaks off the tip, leaving an open pipette. If this has been done properly, the opening of the pipette should be somewhere between one and five microns in radius.

After the tip of the pipette is broken off, though, the end will have jagged edges. This is also detrimental to GUV experiments, as lipid vesicles are fragile and can burst if the jagged edges pierce them. In order to fix this problem, the microforge can also fire polish the edges of the micropipette. By turning the heat on the filament up to around ninety percent of full capacity and bringing the pipette tip close to, but not in contact with, the pipette, the heat from the filament can smooth the edges of the pipette tip. This is not only helpful, but necessary for GUV experiments.

A smooth micropipette is not enough to perform GUV experiments, however, as lipids can adhere to glass. If adhesion occurs, the tension numbers will not be accurate because the membrane will stretch as a result of that adhesion rather than the pressure from the water reservoir. In order to counter adhesion, the micropipettes are coated with a filtered Bovine Serum Albumin (BSA) solution. BSA prevents lipids from sticking to glass.

### *2.3.5 Filling and Coating Pipettes*

The micropipettes must be filled completely before they are connected to the pressure system tubing. The opening of the pipette is so small that it takes a significant amount of force to pump liquid through the tip. Atmospheric pressure alone will not provide enough force. It is also necessary for the pipettes to be completely free of air bubbles; since gas is compressible, raising or lowering the water reservoir when there is an air bubble in the pipette will merely expand or compress the air bubble, rather than move liquid, which is the principal mechanism driving this experiment. It is also nearly impossible to pump an air bubble out the tip of the micropipette.

In order to fill the micropipettes without air bubbles, the backs of fire-polished micropipettes are attached by medical tubing to a vacuum. While there is vacuum inside the pipettes, liquid can be drawn up through the tip of the pipette through capillary action.

Using the same micromanipulator described in section 2.3.3, the pipettes are held in place while attached to vacuum. They are then placed over an improvised three-well chamber. In the first well is pure, deionized water, used to clear the pipette of any residue which may be left over from the fabrication process.

In the second well is the filtered BSA solution. The tip of the pipette is left submerged in the filtered BSA for at least fifteen minutes while simultaneously drawing it in, in order to coat both the inside and the outside of the micropipette tip. Fifteen minutes should be sufficient for coating pipettes, but should also be regarded as a minimum.

The third well contains 0.1 Molar sucrose solution, the same solution used to electroform the GUVs. The same solution is used in order to avoid osmosis across the membrane, which would complicate the pressure calculation. The GUVs are also submerged in the 0.1 Molar sucrose solution when experiments are being performed.

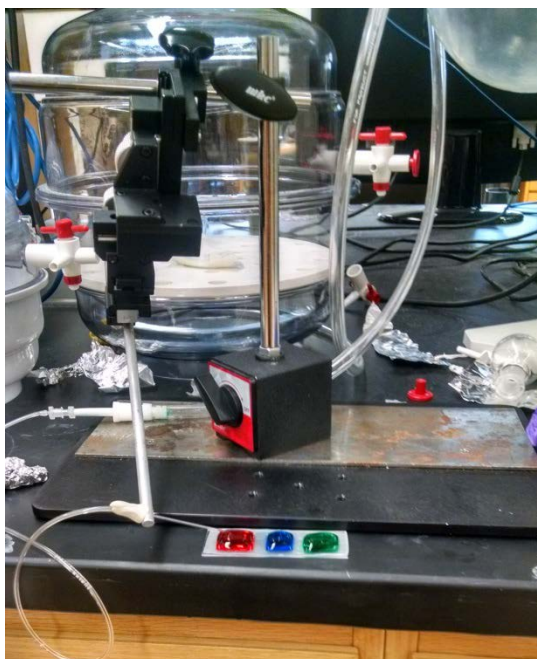


Figure 9: Vacuum Filling System for Micropipettes

A micropipette is woven through a metal rod attached to a micromanipulator. The back of the pipette is attached, by medical tubing, to vacuum, and liquid is drawn up into the pipette through capillary action.



Figure 10: Three-Well Chamber for Filling Pipettes

The left well contains pure, deionized water. The middle well contains filtered BSA solution. The right well contains .1 Molar sucrose solution. Food coloring was added above for illustrative purposes.

## 2.4 Microrheology and Image-Based Tracking

Our technique for measuring diffusive motion in lipid membranes is called passive microrheology. Rheology is the study of how materials flow in response to a force applied to them, and microrheology is just rheology applied to small objects such as cells or, in our case, GUVs. Passive microrheology refers to measurements that rely on the Brownian motion of tracers without an applied external force, as opposed to active microrheology, which depends on some force being applied to the object [21]. The position of particles undergoing Brownian motion or random walks cannot be predicted with 100 percent accuracy, but Brownian motion is a statistical process, meaning that models exist which can predict with some accuracy where the particle will be after one step in relation to where it was in the last step.

In order to measure the diffusion coefficients of lipid domains, we image them under a fluorescent microscope, and then analyze their paths. To create a connected path which we can analyze on a computer, we must calculate the center of the domain in each frame of the video and connect the centers to create a continuous track. Calculating the center of the domain, though, is decidedly non-trivial. To do so, we implement a particle-tracking program written in the MATLAB programming language written by Tristan Hormel, a graduate student in the Parthasarathy Lab [22].

The program takes advantage of the fact that for any given imaged particle, the distribution of its light intensity is radially symmetric about the center. Using this fact, the program uses an algorithm which calculates the point in the image which maximizes its symmetry and calls that point the center. The program needs to perform this calculation for each frame of the video and connect the center of the domain in one

frame to the center of the domain, which has likely moved, in the next frame. The accuracy of the particle tracking obviously depends on the quality and clarity of the images.

By analyzing the continuous path of a lipid domain over time, it is possible to calculate its translational diffusion coefficient. It is also necessary, though, to calculate the size of the lipid domain. In order to calculate the size of a lipid domain, our program uses two thresholds. First is a bandpass filter threshold, which processes a spatial image in the frequency domain, then cuts off the high and low frequencies. What this equates to is an overall smoothing of the image, and a highlighting of the domain edges.

The second filter is based on Otsu's Method, which attempts to threshold image clusters. The method separates foreground pixels from background pixels by assuming they have different intensity values [23]. This is useful for separating domains from the dominant lipid background.

The result of this tracking for a single frame looks like Figure 11 below. The tracking program would produce something similar for each frame to produce continuous tracks for the lipid domains and average sizes for each domain.

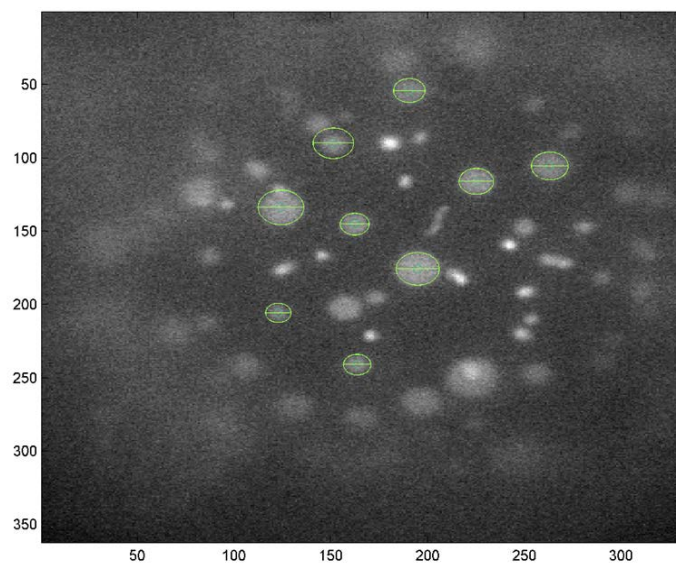


Figure 11: Result of Tracking a Phase-Separated GUV

The green circles display computer estimates for the centers and sizes of the lipid domains. This is the composition I use in my experiments.

## **Chapter 3: Results and Discussion**

### **3.1 Verification of Experimental Approach**

Micropipette aspiration of phase-separated vesicles has worked. Using this approach, I have been able to probe wide ranges of vesicle sizes and membrane tensions. The GUVs I have conducted experiments on have been anywhere from ten to sixty microns in diameter. The membrane tensions I have induced with micropipette aspiration have spanned two orders of magnitude, from under 100  $\mu\text{N/m}$ , to over 2500  $\mu\text{N/m}$ . These numbers indicate that the micropipette aspiration system I constructed, it will be possible to conduct more experiments involving tension in lipid membranes in the future. In fact, another undergraduate is being trained on the system now to carry on these sorts of experiments.

### **3.2 Average Domain Radius and Diffusion Coefficient versus Tension**

It appears that the average size of lipid domains decreases slightly as tension expands. It is also interesting to note that the average domain radius appears to converge as tension increases (see Figure 12).

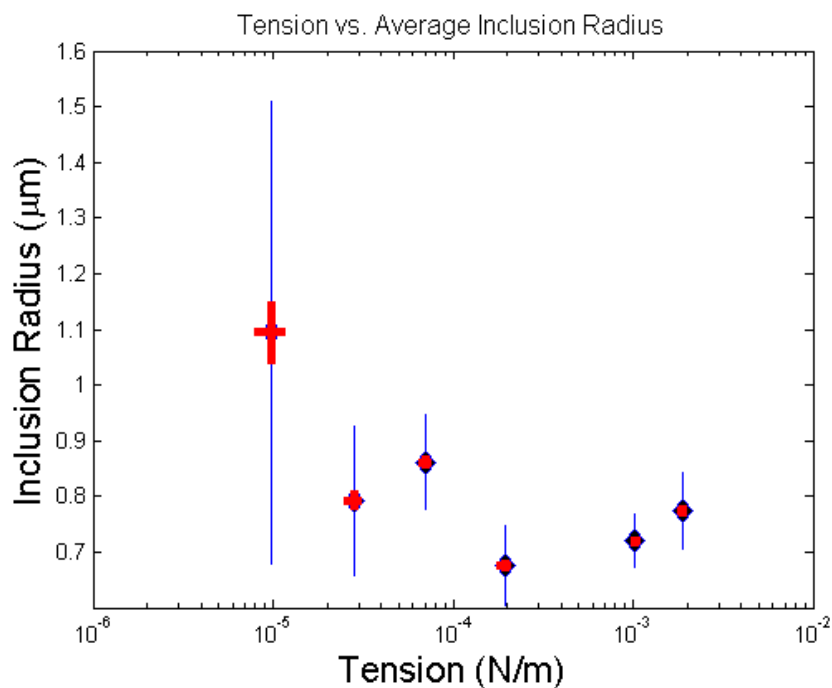


Figure 12: Membrane Tension vs. Average Domain Radius

There appears to be a slight decrease in the average lipid domain radius as membrane tension increases. The average radius also appears to converge at high tension.

At lower tensions, lipid domain radii, on average, spanned from about 0.9 to 2 microns in radius, while at higher tensions, lipid domain radii spanned from about 0.7 to 0.8 microns.

The average diffusion coefficient appears to increase as membrane tension increases. Also, the spread in the diffusion coefficients seems to decrease at high membrane tensions (see Figure 13). In fact, the data is quite convincing

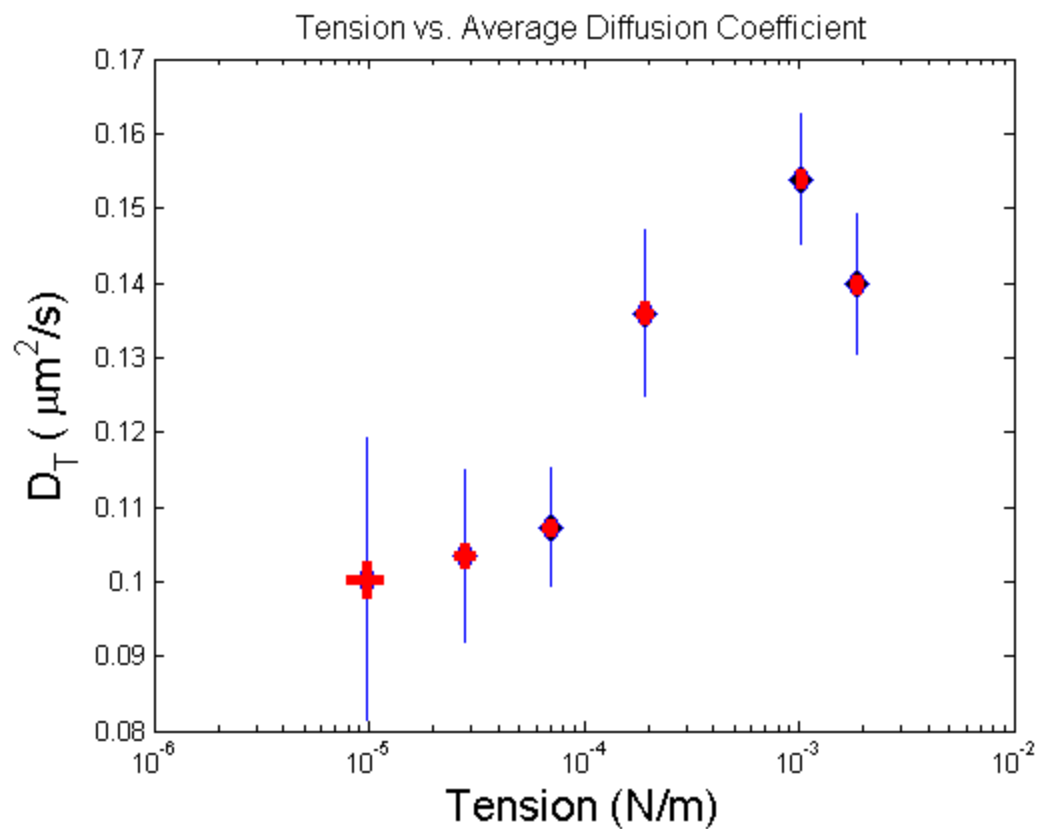


Figure 13: Membrane Tension vs. Average Diffusion Coefficient

The average diffusion coefficient appears to increase as membrane tension increases, and the spread appears to decrease at high tensions.

### 3.3 Viscosity versus Membrane Tension

The question this thesis set out to answer was what effect, if any, tension has on lipid membrane viscosity. After analyzing the data, it appears that membrane viscosity decreases as tension increases. It also appears that the spread in membrane viscosity decreases significantly at high tensions (see Figure 14).

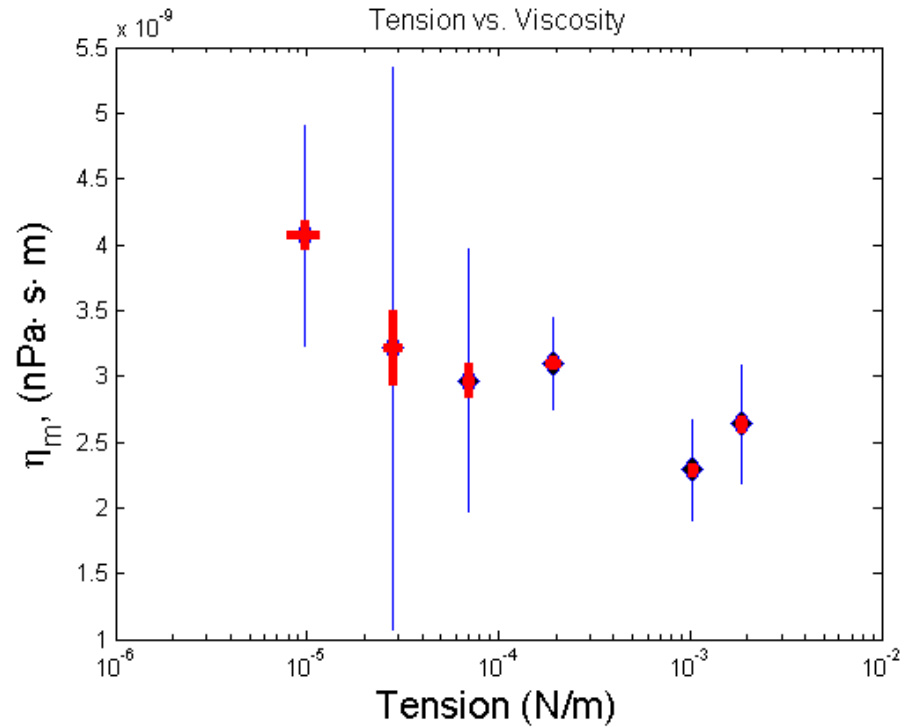


Figure 14: Membrane Tension vs. Viscosity

It appears that viscosity decreases as membrane tension increases, which is in line with my original hypothesis. It also appears that the spread in membrane viscosity decreases significantly at high tensions. The blue bars represent combined standard deviation, while the red bars are the standard error. These points represent sixty GUVs

### 3.4 Conclusions and Implications

The micropipette aspiration system I designed is effective for performing tension experiments on lipid vesicles. Using it, I have shown that lipid membrane viscosity decreases as tension increases. This could have interesting implications for biological processes which involve cell membranes stretching, such as metastasizing cancer cells or cells undergoing division. The results of this experiment certainly warrant further exploration into lipid membranes under tension.

This is the first time tension-mediated changes in membrane viscosity have been measured. The intuitive explanation for the decrease in viscosity is that tension stretches

out the membrane, leading to more space between lipids, making motion in the membrane easier. Though it is impossible to confirm this explanation without seeing single lipids diffusing, the data at least supports the explanation.

Future experiments which might involve the micropipette aspiration system include spanning large ranges of tension on the same vesicle, or testing the effect of temperature on tension and membrane viscosity. It is known that both temperature and tension affect the phase-transition behavior of mixed-lipid vesicles, and it would be interesting to create a phase diagram which takes the two variables into account.

## **Appendix A: Making Giant Unilamellar Vesicles**

The Parthasarathy Lab protocol for making Giant Unilamellar Vesicles is based on both Tristan Ursell's electroformation protocol and the Veatch-Keller protocol.

### **Materials**

- Indium-tin-oxide (ITO) coated glass slide
- Silicone gasket material
- Binder clips
- Conductive Copper tape

### **Procedure**

1. Cut an ITO glass slide in half. Place copper tape so that the length of it hangs significantly off the edge of the conducting side of the glass, and the width of it hangs only slightly off the glass. The conducting side of the glass can be found by testing it for resistance using a multimeter.
2. Clean ITO glass with ethanol and DI water. First rinse the ITO glass, then gently dab on ethanol using a Kim wipe, then repeat the ethanol and water rinse. Dry using nitrogen gas from tank.
3. Cut the silicone gasket material into a U-shape the size of one of the glass slide halves. Both halves will be held together with the silicone U placed in between
4. Clean the silicone gasket with plenty of soap and water.
5. For phase-separated GUVs, place the clean and dry ITO glass slides on a hot plate for at least ten minutes at 200 degrees Celsius.
6. After ten minutes, remove the glass slides and deposit your lipid composition onto the slides using a lipid syringe. The lipid syringe is a 10  $\mu\text{L}$  syringe which should be cleaned out prior to use with chloroform. At most, 5  $\mu\text{L}$  of lipid solution should be deposited onto the glass.

7. Place the glass slides in the desiccator and cover loosely with a piece of aluminum foil to block out the light. Turn on the vacuum and leave the slides covered for at least thirty minutes.
8. When thirty minutes have passed, form a capacitor by sandwiching the silicone U with the ITO glass slides. The lipid side of the slides should be facing each other. The slides can be held together with a binder clip, leaving the opening of the U uncovered
9. Backfill the capacitor with hydration solution using a syringe. The hydration solution is typically 0.1 M sucrose.
10. Seal the opening of the U with another binder clip.
11. Wire the capacitor to a function generator using alligator clips attached to the copper tape.
12. Set the function generator to produce a 10 Hz sine wave, with  $V_{\text{rms}}$  (root-mean-square) of 1.2 Volts, 0 Volt offset. Leave the slides attached and covered from light for two to three hours. Three hours seems to produce better GUVs
13. For phase-separated vesicles, the slides should also remain heated above their phase transition temperature for the entirety of the electroformation
14. When the two to three hours have passed, turn off the function generator and extract the vesicle solution using a designated vesicle syringe.
15. Store the vesicle solution at 4 degrees Celsius or, if making phase-separated vesicles, at room temperature or above.
16. GUVs are best to use within two to three days of formation
17. Glass slides can be re-used two more times if the cleaning protocol is followed after the vesicles have been extracted. After three uses, the slides should be discarded, and new glass should be used.

## Bibliography

- [1] Nag, K. (2008). Structure and dynamics of membranous interfaces. Hoboken, N.J.: Wiley.
- [2] Phillips, R., Kondev, J., & Theriot, J. (2009). *Physical biology of the cell*. New York, NY: Garland Science.
- [3] Parthasarathy, R., & Groves, J. (n.d.). Curvature and spatial organization in biological membranes. *Soft Matter*, 24-24
- [4] Grakoui A1, Bromley SK, Sumen C, Davis MM, Shaw AS, Allen PM, Dustin ML, *Science*, 1999 Jul 9;285(5425):221-7
- [5] Singer, S., & Nicolson, G. (1972). The Fluid Mosaic Model Of The Structure Of Cell Membranes. *Science*, 175, 720-731
- [6] Saffman, P., & Delbruck, M. (1975). Brownian Motion in Biological Membranes. *Proceedings of the National Academy of Sciences*, 72(8), 3111-3113.
- [7] B. D. Hughes, B. A. Pailthorpe and L. R. White (1981). The translational and rotational drag on a cylinder moving in a membrane. *Journal of Fluid Mechanics*, 110, pp 349-372
- [8] Diz-Muñoz, A., Fletcher, D. A., & Weiner, O. D. (2013). Use the force: Membrane tension as an organizer of cell shape and motility. *Trends in Cell Biology*, 23(2), 47–53
- [9] Raucher, D., & Sheetz, M. P. (2000). Cell Spreading and Lamellipodial Extension Rate Is Regulated by Membrane Tension. *The Journal of Cell Biology*, 148(1), 127–136.
- [10] Schweitzer, Y., Lieber, A. D., Keren, K., & Kozlov, M. M. (2014). Theoretical Analysis of Membrane Tension in Moving Cells. *Biophysical Journal*, 106(1), 84–92. doi:10.1016/j.bpj.2013.11.009
- [11] Houk, A. R., Jilkine, A., Mejean, C. O., Boltyanskiy, R., Dufresne, E. R., Angenent, S. B., ... Weiner, O. D. (2012). Membrane tension maintains cell polarity by confining signals to the leading edge during neutrophil migration. *Cell*, 148(1-2), 175–188. doi:10.1016/j.cell.2011.10.050
- [12] Iscla, I., & Blount, P. (2012). Sensing and Responding to Membrane Tension: The Bacterial MscL Channel as a Model System. *Biophysical Journal*, 103(2), 169–174. doi:10.1016/j.bpj.2012.06.021

- [13] Veatch, S., & Keller, S. (2003). Separation of Liquid Phases in Giant Vesicles of Ternary Mixtures of Phospholipids and Cholesterol. *Biophysical Journal*, 85, 3074-3083
- [14] Veatch, S., & Keller, S. (2002). Organization in Lipid Membranes Containing Cholesterol. *Physical Review Letters*, 89(26)
- [15] Chen, D., & Santore, M. (2014). Large effect of membrane tension on the fluid-solid phase transitions of two-component phosphatidylcholine vesicles. *Proceedings of the National Academy of Sciences*, 111(1), 179-184.
- [16] Marsh, D. (2010). Liquid-ordered phases induced by cholesterol: A compendium of binary phase diagrams. *Biochimica Et Biophysica Acta (BBA) - Biomembranes*, 688-699.
- [17] Hormel, T., Kurihara, S., Brennan, M., & Parthasarathy, R. (2014). Measuring Lipid Membrane Viscosity using Rotational and Translational Particle Diffusion. *Physical Review Letters*, 112(18), 188101-5.
- [18] De Gennes, P., Brochard-Wyart, F., & Quere, D. (2004). *Capillarity and Wetting Phenomena: Drops, Bubbles, Pearls, Waves*. New York, NY: Springer
- [19] Portet, T., Gordon, S. E., & Keller, S. L. (2012). Increasing Membrane Tension Decreases Miscibility Temperatures; an Experimental Demonstration via Micropipette Aspiration. *Biophysical Journal*, 103(8), L35–L37.
- [20] Hochmuth, R. (2000). Micropipette aspiration of living cells. *Journal of Biomechanics*, 33, 15-22.
- [21] Chen, D., Wen, Q., Janmey, P., Crocker, J., & Yodh, A. (2010). Rheology of Soft Materials. *Annual Review of Condensed Matter Physics*, 301-322.
- [22] Parthasarathy, R. (2012). Rapid, accurate particle tracking by calculation of radial symmetry centers. *Nature Methods*, 9(7), 724-726.
- [23] Otsu, N. (1979). A Threshold Selection Method from Gray-Level Histograms. *IEEE Transactions on Systems, Man, and Cybernetics*, 9(1), 62-66.